Moisture Dependent Diffusion and Shrinkage in Yam during Drying.

Amankwah, E. A., Dzisi, K. A., van Straten, G., & van Boxtel, A. J. B.

Moisture dependent diffusion and shrinkage in yam during drying

E.A. Aamankwah[1,2], K.A. Dsizi[2], G. van Straten[1], A.J.B. van Boxtel[1]

[1] Biobased Chemistry and Technology, Wageningen University Research.
POBox 17, 6700 AA, Wageningen, the Netherlands
[2] Food Science and Technology and Biochemistry and Biotechnology Departments,
Kwame Nkrumah University of Science and Technology,
Kumasi, Ghana

Abstract

Crank's analytical approximations for Fick's diffusion equation were used to investigate the effect of moisture dependent sample thickness and diffusivity on the drying behavior of yam (*Dioscoreaceae rotundata*) cubicles. Drying and shrinkage experiments were separately conducted at temperatures of 30, 40 and 50ºC in a cabinet drier. The comparative study of moisture dependent shrinkage and moisture dependent diffusivity justifies the interdependence of diffusivity and shrinkage due to water loss during drying. The behavior for yam is best explained by a combination of fractal moisture dependent shrinkage and moisture dependent diffusion, describing both the drying and rate curves better with good prediction of the high moisture regions. This assertion was reached as a result of low mean square error, standard error, percentage relative deviation, Akaike's Information Criterion and high coefficient of determination. The results may indicate a varying mobility of water in food matrix of different moisture content in the multilayer and monolayer regimes.

Keywords: Yam (*Dioscoreaceae rotundata*), drying curves, water transport, effective diffusion

1. Introduction

Yam, a delicacy and a major source of food supply for many African, Asian and Latin American countries, has a moisture content of about 70% when harvested, which make yam perishable [1] This can be prevented by drying into powders and storage under appropriate conditions. The powders are incorporated into soups, baby foods or processed into a thick viscous diet called Amala in Nigeria or Fufu in Ghana. Yam powder is obtained from yam cubicles which are dried in a traditional way like open sun drying or by using industrial or solar dryers. During drying, shrinkage occurs. To advance drying technology, it is essential to quantify and analyze the drying characteristics of yam cubicles, not neglecting the shrinkage factor.

Torres et al. [2] report about the drying characteristics of two yam species (*Dioscoreaceae alata*) by using a classical model approach. The use of the Page equation is a semi-empirical approach and does not reflect the diffusion behavior that occurs in many food products as formulated by [3, 4, 5] who have shown a linear relationship between moisture and shrinkage. Sjöholm and Gekas [6] have shown a linear relationship between D_{eff} and moisture content during apple drying as a consequence of volume change with moisture content. The change of moisture content in these products is given by Fick's second law:

$$\frac{dX(t,x)}{dt} = \frac{d}{dx} D \frac{dX(t,x)}{dx} \quad (1)$$

with $X(t,x)$ the moisture content (kg water/kg solids) as a function of time (t) and position (x) in the product compared to the center. D is the effective diffusion coefficient (m^2/s).

Crank [7] provided analytical solutions of the diffusion equation for standard shaped products. For a product with an uniform initial moisture concentration (X_0), negligible external resistance and time invariant diffusion coefficient the analytical solutions for the average moisture content in an infinite sized slab is given as:

$$MR(t) = \frac{X(t) - X_e}{X_o - X_e} = \frac{8}{\pi^2} \sum_{n=0}^{\infty} \frac{1}{(2n+1)^2} exp\left(-\frac{(2n+1)^2 \pi^2 D}{L^2} t\right) \quad (2)$$

With $MR(t)$ the moisture ratio, $X(t)$ the actual averaged moisture content, X_0 the initial moisture content, X_e the equilibrium moisture content at the end of drying, all in kg water/kg solids and $L\ (m)$ the thickness of the slab.

Equation 2 represents a series of terms and writing the first 3 terms out ($n = 0{,}1$ and 2) gives

$$MR(t) = \frac{8}{\pi^2} exp\left(-\frac{\pi^2 D}{L^2} t\right) + \frac{8}{9\pi^2} exp\left(-\frac{9\pi^2 D}{L^2} t\right) + \frac{8}{25\pi^2} exp\left(-\frac{25\pi^2 D}{L^2} t\right) + .. \quad (3)$$

The time scales of the successive terms differ strongly, i.e. the time scale of the third term is very short, for the second term, longer but still fast and the expression is dominated by the time scale of the first term. Together with a decreasing pre-exponential factor for each term, in practice just one or two terms suffice ($n = 0\ and\ 1$), leading to Eq. 4 as a suitable basis for the interpretation of drying curves ($n = 0\ and\ 1$).

$$MR(t) = \frac{8}{\pi^2} exp\left(-\frac{\pi^2 D}{L^2} t\right) + \frac{8}{9\pi^2} exp\left(-\frac{9\pi^2 D}{L^2} t\right) \quad (4)$$

Often only one term is used as reported by [8,9,10,11,5].

In our experiments on drying of yam cubicles with a limited size, we observed systematic deviations between the data and fitted curves based on Eq. 4. Assuming that moisture transport for yam is diffusion limited, these deviations can be a result of the following issues: (i) the geometry of the cubicles does not satisfy the conditions for infinite sized slabs, (ii) moisture transport is affected by shrinkage [12], or (iii) the effective diffusion coefficient is not constant [13].

In this work we perform a step-wise analysis to understand the observed deviations between the data and fits for Eq. 4. To check the role of the geometry and size of the particles an analysis with computational fluid dynamics is performed. The role of shrinkage is investigated by using the concepts of volume reduction [6] and the effect of fractal change of thickness [14]. Ruiz-Lopez and Garcia-Alvarado [13] relate the diffusivity of water in the product matrix to moisture content. In line with their observations a moisture dependent diffusion coefficient is evaluated in this work.

2. Materials and Methods

2.1. Yam species and sample preparation

Yam tubers, *Dioscoreaceae rotundata* cultivar *Dente,* were precisely cut into discs of 10 mm thickness and subsequently the discs were further cut into square dimensions of 30 mm by 30 mm. The dimensions of the samples were measured using digital calipers (model: 01407A, NEIKO, USA) of 0.02 mm accuracy.

2.2. Shrinkage and moisture measurements

In separate experiments on shrinkage, ten fresh yam cuts (3x3x1cm) were placed in the drying chamber and dried at 30, 40 and 50°C. Before and after drying for 2, 4, 6, and 15 hours for all temperatures, plus 19, 42 and 72 hours for 50, 40 and 30 °C, respectively and, 5 samples (replicates) were randomly selected from the drying chamber. For each sample cubicle, the side thickness (S_T) and side lengths (S_L) were determined with the digital calipers at the four sides of the sample, while the center thickness (C_T) was measured three times within the neighborhood of the center of the sample. The average values each of the S_T, $\mathrm{S_L}$ and $\mathrm{S_T}$ ere calculated. After the size measurements the corresponding moisture content of the samples were determined.

According to [14] the relative sample thickness and sample volume are related to each other by an exponential relation with fractal dimensional exponent (z) as shown in Eq. 5:

$$\frac{L_i}{L_0} = \left[\frac{V_i}{V_0}\right]^{1/z} \tag{5}$$

With V_0 and L_0 respectively the initial sample volume (mm^3) and thickness (mm), V_i and L_i the volume and thickness of the sample at the sampling moments during drying. The thickness of the sample is the average value from the four measured side thicknesses (S_T) and the center thickness (C_T):

$$L_i = \left[\frac{4S_T + C_T}{5}\right] \tag{6}$$

The circular deformation from the sides to the center at the top and bottom surface of the sample is considered as a parabolic form. With symmetrical surfaces, the actual volume of the product is then the volume of a square product V_{sqr} minus the volume of the parabolic indentions V_{par}:

$$V_i = V_{sqr} - 2V_{par} = S_L^2 S_T - 2(0.5\pi r^2 h) \tag{7}$$

With $r = \frac{S_L}{2}$ the radius of parabola basis and $h = \frac{S_T - C_T}{2}$ the height of the parabola.

2.3. CFD- calculations

In COMSOL two geometries of product cubicles (3×3×1 cm) were defined and Ficks diffusion equation was applied to these geometries. Simulations were performed with a diffusion coefficient of 2.5×10^{-10} m^2/s. The initial condition for water content throughout the geometry was set to 1.0 kg/m^3 and at the boundaries of the geometry at 0.0 kg/m^3. Drying in the first geometry corresponds to an infinite slab by blocking water transport through the side surfaces which results in water transport through only the top and bottom surface. The second geometry concerned the actual drying behavior by moisture transport through all surfaces. The results were evaluated by fitting Eq. 4 to the simulated moisture content as a function of time.

2.4. Drying procedure and equipment

The dryer system was made up of a fan, heating element and drying chamber. Ambient air at a speed of 2.6 m/s reaches the heating element by a fan (accuracy ±0.05 m/s) through a controlled valve. The temperatures of the heated air and in the chamber were measured with K-type thermocouples (accuracy ±0.1°C). The relative humidity of the inlet air to the dryer was determined by a relative humidity sensor of accuracy ±0.2%RH. The inlet air enters the dryer at the bottom side and leaves at the top side (See Figure 1).

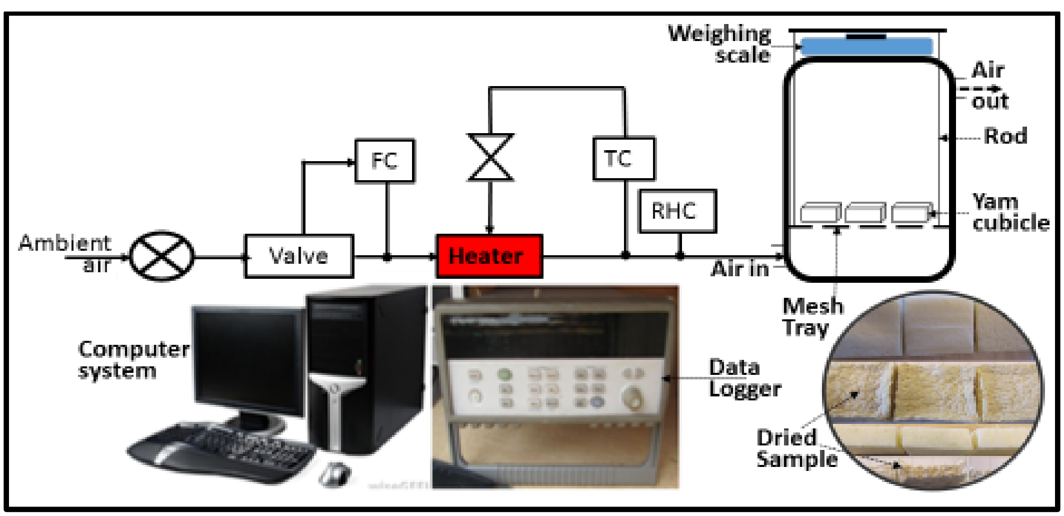

Figure 1 Schematic overview of the drying equipment with flow control (Fl Ctl) and temperature control (T Ctl), processor and data logger

The air flow and air temperature were kept constant through PID controllers. At steady state of temperature and air speed, yam cuts (3x3x1cm) weighing between 170-180g were carefully placed on a wire mesh tray in the drying chamber (Figure. 1). The wire mesh tray is connected to a weighing scale (Mettler Toledo, PM250, Switzerland) to automatically read the changes in weight during drying. An Agilent data logger (model: 34970A, USA) logs and stores the drying air temperatures, air speed, relative humidity and changes in the sample weight by using a Labview interface. All data were recorded within intervals of 2 seconds each and repeated for drying air temperatures of 30, 40 and 50ºC.

2.5. Statistical analysis of data

Nonlinear regression in Matlab was used for parameter estimation of the models to the experimental data. The extent of variation between experimental data and model was determined with the statistical performance indicators:

Standard error:
$$SE = \sqrt{\frac{\sum_{i=1}^{N_e}(Residuals)^2}{N_e - N_p}} \quad (8)$$

Percent average relative deviation:
$$PRD(\%) = \frac{100}{N_e}\sum_{i=1}^{N_e}\left(\frac{|Residuals|}{X}\right) \quad (9)$$

The mean square error (MSe)
$$MSe = \frac{\sum_{i=1}^{N_e}(Residuals)^2}{N_e} \quad (10)$$

Where the residuals are the differences between the observed and predicted data. and X is the observed moisture content value. In general, a better fit is obtained with more parameters, but the improvement must be worth-while. Akaike’s Information Criterion (AIC) is especially suitable for comparing models with a different number of parameters. The criterion is defined by

$$AIC = 2N_p + N_e \ln(V(\hat{\mathbf{p}})) \quad (11)$$

based on the likelihood function, but ignoring the constant term $-N_e \ln(N_e) - N_e \ln(2\pi) - N_e$. The model with the lowest AIC is preferred. Here $V(\hat{\boldsymbol{p}})$ is the sum of squares errors, N_p is the number of parameters of a particular model, and N_e is the number of experimental data points. All data were processed and evaluated using the Matlab software.

3. Results and Discussion

3.1. Shrinkage

Table 1 shows the mean dimensions of the yam cubicles and its corresponding moisture content in time. Shrinkage is highest in the center of the cubicle and is temperature dependent. The percentage shrinkage is between 44-64% in the center with highest shrinkage recorded at 50ºC From the data in Table 1 first the thickness and volume were calculated according Eqns. 6 and 7 and next the results were transformed to the relative thickness ($L_c = L_i/L_0$) and relative volume ($V_c = V_i/V_0$) by dividing with the initial values at start of the experiment. These results are given in Table 2.

Table 1 Measured dimensions of yam cubicles and moisture content for drying at 30, 40 and 50°C

Time (h)	30 °C				40 °C				50 °C			
	S_L (cm)	S_T (cm)	C_T (cm)	X(db)	S_L (cm)	S_T (cm)	C_T (cm)	X(db)	S_L (cm)	S_T (cm)	C_T (cm)	X(db)
0	3.00	1.00	1.00	2.330	3.00	1.00	1.00	2.330	3.00	1.00	1.00	2.330
2	2.93 (0.019)	0.91 (0.037)	0.92 (0.032)	1.758	2.84 (0.030)	0.90 (0.021)	0.89 (0.022)	1.390	2.83 (0.073)	0.86 (0.017)	0.85 (0.012)	1.12
4	2.85 (0.065)	0.88 (0.032)	0.87 (0.043)	1.589	2.76 (0.04)	0.83 (0.024)	0.78 (0.035)	1.104	2.7 (0.053)	0.8 (0.024)	0.64 (0.011)	0.77
6	2.78 (0.049)	0.87 (0.032)	0.79 (0.045)	1.132	2.69 (0.047)	0.79 (0.029)	0.72 (0.031)	1.055	2.6 (0.026)	0.79 (0.039)	0.56 (0.045)	0.52
15	2.74 (0.046)	0.84 (0.031)	0.62 (0.027)	0.625	2.61 (0.057)	0.74 (0.029)	0.56 (0.024)	0.400	2.5 (0.042)	0.7 (0.020)	0.48 (0.028)	0.254
19	-	-	-	-	-	-	-	-	2.48 (0.036)	0.68 (0.019)	0.36 (0.032)	0.045
47	-	-	-	-	2.58 (0.029)	0.70 (0.02)	0.50 (0.035)	0.140	-	-	-	-
72	2.71 (0.025)	0.83 (0.026)	0.56 (0.025)	0.170	-	-	-	-	-	-	-	-
%Shr	10	17	44	-	14	30	50	-	17	32	64	-
Sdv_{ave}	0.0408	0.0316	0.0344		0.0406	0.0246	0.029		0.046	0.0238	0.0272	
Stdev (Stdev)	0.0187	0.00391	0.00915		0.01180	0.00427	0.00660		0.01799	0.00887	0.01509	

() = standard deviation over 5 replicates, Shr = shrinkage, Sdv_{ave} = average of standard deviation, Stdev (Stdev) = Standard deviation of the standard deviation

Table 2 Relative volume (V_c) and thickness (L_c) derived from the product dimensions (Table 1) and product moisture content ($X(t)$) during drying at temperatures ranging between 30-50 ºC

Moisture content X (kg/kg)	Relative thickness L_c (-)	Relative volume V_c (-)
30 ºC		
2.33	1.00	1.00
1.76	0.91	0.87
1.59	0.88	0.79
1.13	0.85	0.72
0.63	0.80	0.63
0.17	0.78	0.59
40 ºC		
2.33	1.00	1.00
1.39	0.90	0.80
1.10	0.82	0.69
0.66	0.78	0.61
0.40	0.70	0.51
0.14	0.66	0.46
50 ºC		
2.33	1.00	1.00
1.12	0.86	0.76
0.77	0.77	0.60
0.52	0.74	0.52
0.25	0.66	0.43
0.05	0.62	0.38

Linear regression of relative thickness (L_c) against moisture content (X) at temperatures 30, 40 and 50 ºC respectively gave the combined linear equations as:

$$Lc(X,T) = (0.0033\mathrm{T} + 0.0105)\mathrm{X} + 0.8870 - 0.0054\mathrm{T} \tag{12}$$

Equation 5 relates the relative thickness (L_c) and relative volume (V_c) through the fractal coefficient (z). Figure 2 presents the double logarithmic plot of relative thickness and volume for all data from Table 2, which results in average fractal factor, $z = 1.98$. This value is in the upper range of the values found by [14] and (z=1.4-1.8) and indicates a relative strong contribution of the sample thickness to the volume (See Figure 2).

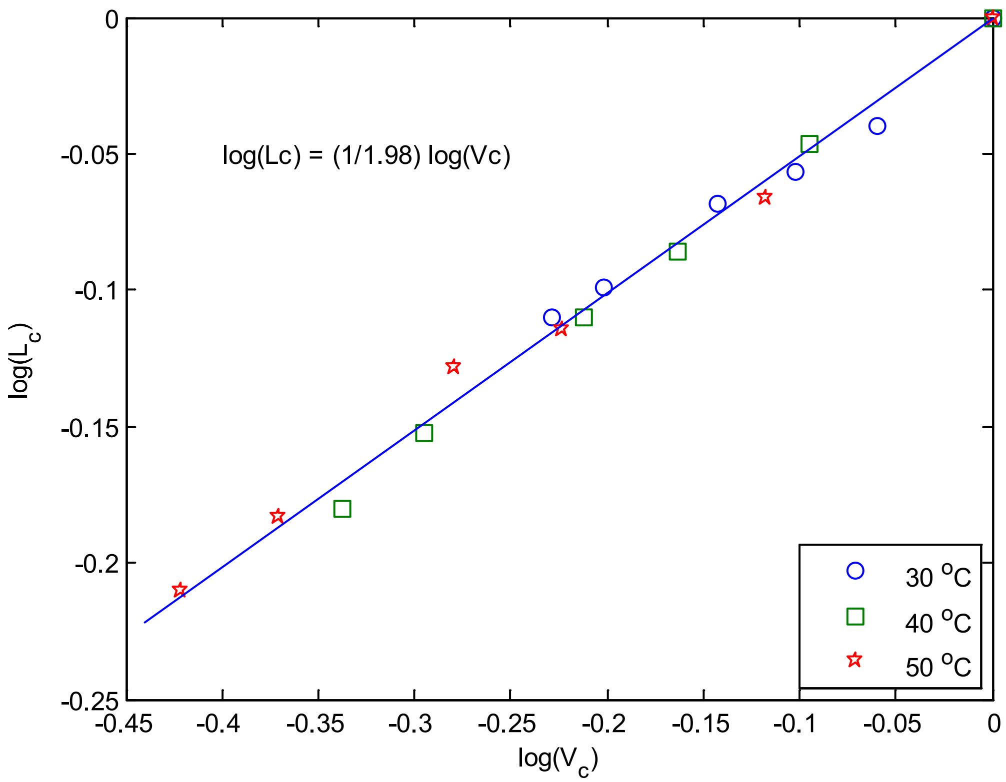

Figure 3 Logarithm of volume change (V_c) against logarithm of thickness change (L_c) for temperatures ranging between 30-50 ºC.

The yam cubicle dimensional reduction during drying represented by the relative volume from Table 2 at temperatures 30-50ºC showed non-linear relationships with moisture content (X). Regression analysis of $\log(V_c)$ as a function of $X - Xo$ is given as:

$$\log(V_c) = SX - SX_0 \qquad (13)$$

Where S is the slope, X_0 is the initial moisture content, X is the moisture content in time, both given as kg water/kg dry matter. The combination gives

$$\log(Vc) = (0.0038\mathrm{T} - 0.0012)\ X - \ 0.0065\mathrm{T} + 0.0738 \qquad (14)$$

The expression for the final relative thickness is then:

$$\frac{L}{L_0} = L_c = 10^{\frac{[(0.0038\mathrm{T}-0.0012)X-(0.0065\mathrm{T}+0.0738)]}{z}} \qquad (15)$$

Both equation 12 and 15 give an expression for the relative thickness as a function of moisture content and temperature. The difference between both equations arises from the applied procedure to link the relative thickness to the moisture content. Equation 12 is based on direct regression between thickness and moisture content, while equation 15 is based on regression between product volume and moisture content.

3.2. Drying and drying rate curves

Figure 3 (top) shows the drying curves of the observed data of yam cubicles at temperatures of 30, 40 and 50°C. The figure shows the well-known trends for drying curves, with a decreasing moisture ratio over time and shorter drying times for higher temperatures. From the raw data the drying rate was derived and expressed as a function of the moisture ratio (Figure 3 (bottom)). Figure 3 (bottom) shows that the drying rate increases with moisture ratio and with steeper slope for higher temperatures. The plots show two main phases of rates which can, at first sight, be approximated by linear functions as: 1) a linear function for the range 0 - 0.5 and a linear function for the range above 0.5. Jannot et al. [15] reported of 3 phases for banana. In the next part these phases section are analyzed by Crank's approximation for Fick's second law.

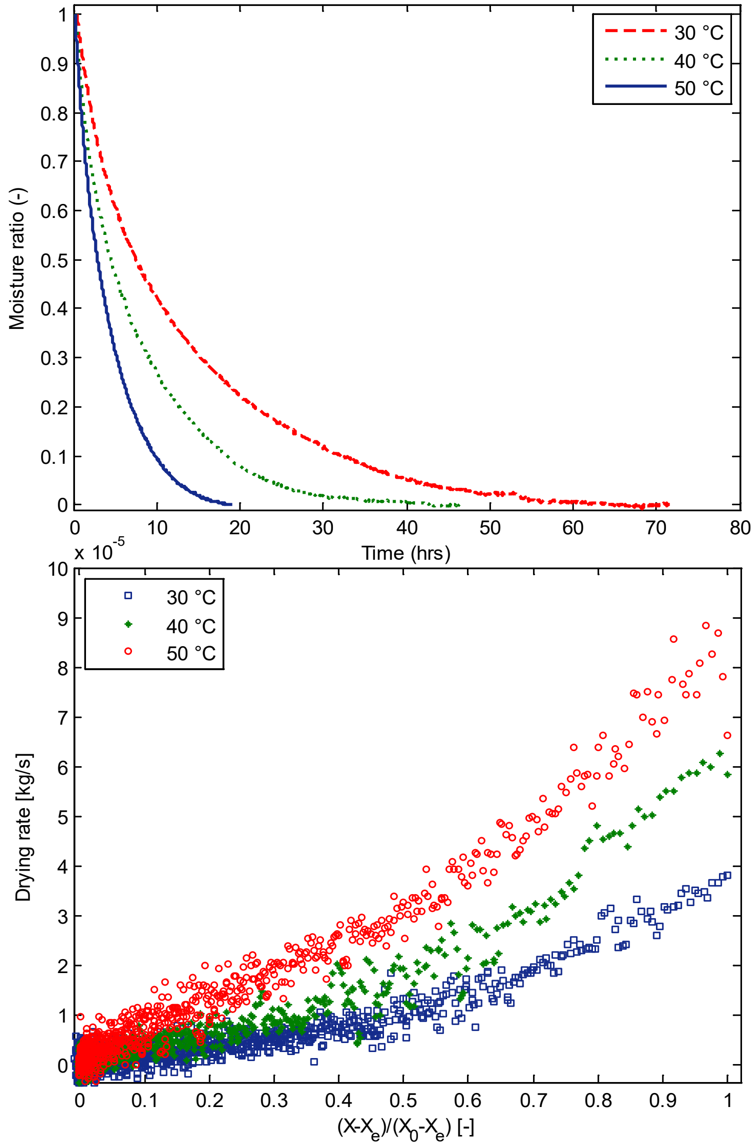

Figure. 3 Experimental data of moisture ratio against time (top) and drying rate against moisture (bottom) of yam at different temperatures

3.3.CFD-results

Figure 4 represents the distribution for the moisture ratio in product samples with moisture transport through all product edges at 20000 and 50000 seconds. The distribution, with a gradual decrease of moisture towards the edges of the product, is a characteristic example for diffusional mass transport in a sample with limited dimensions. For products that behave as an infinite slab there is only a gradient towards top and bottom of the sample.

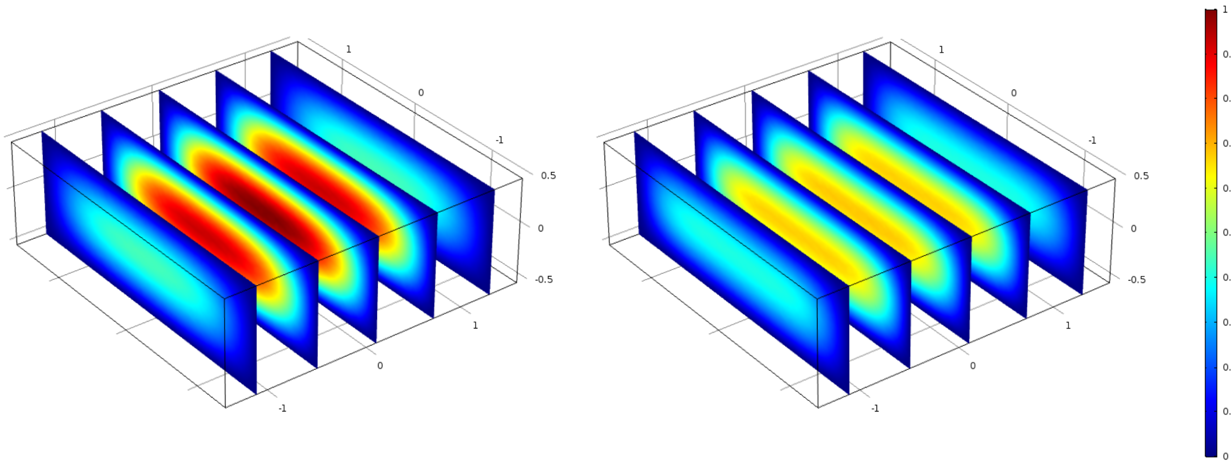

Figure 4 Profile of moisture ratio in the product samples with transport through all side planes at 20000 and 50000 seconds of drying.

Like in Figure 3, CFD generated data of the drying rate for the two geometries are plotted against the moisture ratio in Figure 5 (top: transport through only bottom and top and satisfying the properties of an infinite slab, bottom: moisture transport through all sides). Comparison of the results shows that the drying rate in the second geometry is above that of the first geometry, which is evident due to the larger product surface available for drying. Applying the three term model (Eq. 3) to fit the drying curve ($X(t)$ as a function of time resulted in the dashed lines in both graphs. Overall, the drying rate from the three term model is in both cases very close to the data, the main difference is in the region of the high moisture ratio. The performance in the high moisture region could be slightly improved by adding more terms. The estimated diffusion coefficient for the first geometry corresponds to that used in the simulations to generate the data. For the second geometry the estimated diffusion coefficient is higher due to the larger drying rates that result from the extra moisture transferring surfaces. These results show that, with a higher effective diffusion coefficient, Crank's approximation can also be applied for the considered particles with moisture transport through the side surfaces. Moreover, the different phases in the drying rate in Figure 3 are not result of the rather small dimensions of the particles used in the experiments.

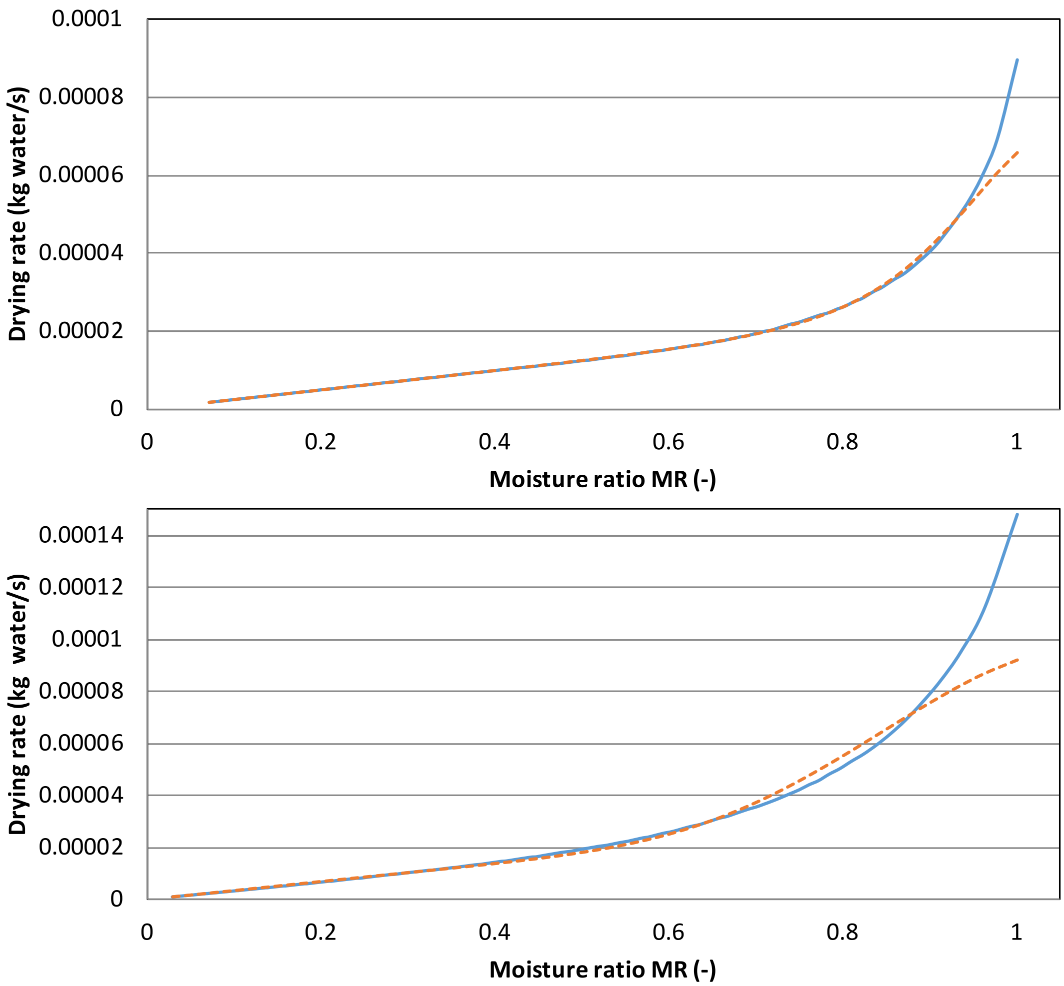

Figure 5. Comparing CFD generated data for a geometry with moisture transport through the top and bottom surface (top), and a geometry with moisture transport through all sides (bottom). Drawn line CFD data, dashed line approximation with the Crank's approximation with three terms.

3.4. Fitting drying curves to data

The form of the drying rate curves for the data generated by CFD and the measured data given in Figure 3 (bottom) have a large similarity and therefore the measured drying curves were fitted with the Eq. 4 with 2 terms. The noise in the measured data was too high for a statistical meaningful application of 3 terms (Eq. 3). To compensate partly for the effects of higher terms, the coefficient of the second term in the right hand side of Eqn. (4) is considered as a parameter (Eq. 16).

Non-linear
$$MR(t) = \mathrm{a}\, exp\left(-\frac{\pi^2 D(X)}{L(X)^2}t\right) + p\, exp\left(-\frac{9\pi^2 D(X)}{L(X)^2}t\right) \quad (16)$$

At first, Eq. 16 is fitted to the data with fixed values for the diffusion coefficient D and sample thickness L. Figure 6 shows measured and model curves of the non-linear approximation for the diffusion equation (where $\mathrm{a} = \frac{8}{\pi^2}$). The obtained parameters and the statistics of the fit are given in Table 2.

Figure 6 (top) represents moisture ratio as a function of time while the bottom figure represents the drying rate as a function of moisture ratio at constant slab thickness and diffusion coefficient. The figures show systematic errors in the models, while the drying rate curves reflect a drastic deviation of the models from the observed data. However, it is able to produce the two phases as observed in Figure 4 (bottom). The deviation of the drying rate curve (Figure 6, bottom) can possibly be a result from 1) product shrinkage, 2) a moisture dependent diffusion coefficient, or 3) a combination of these two.

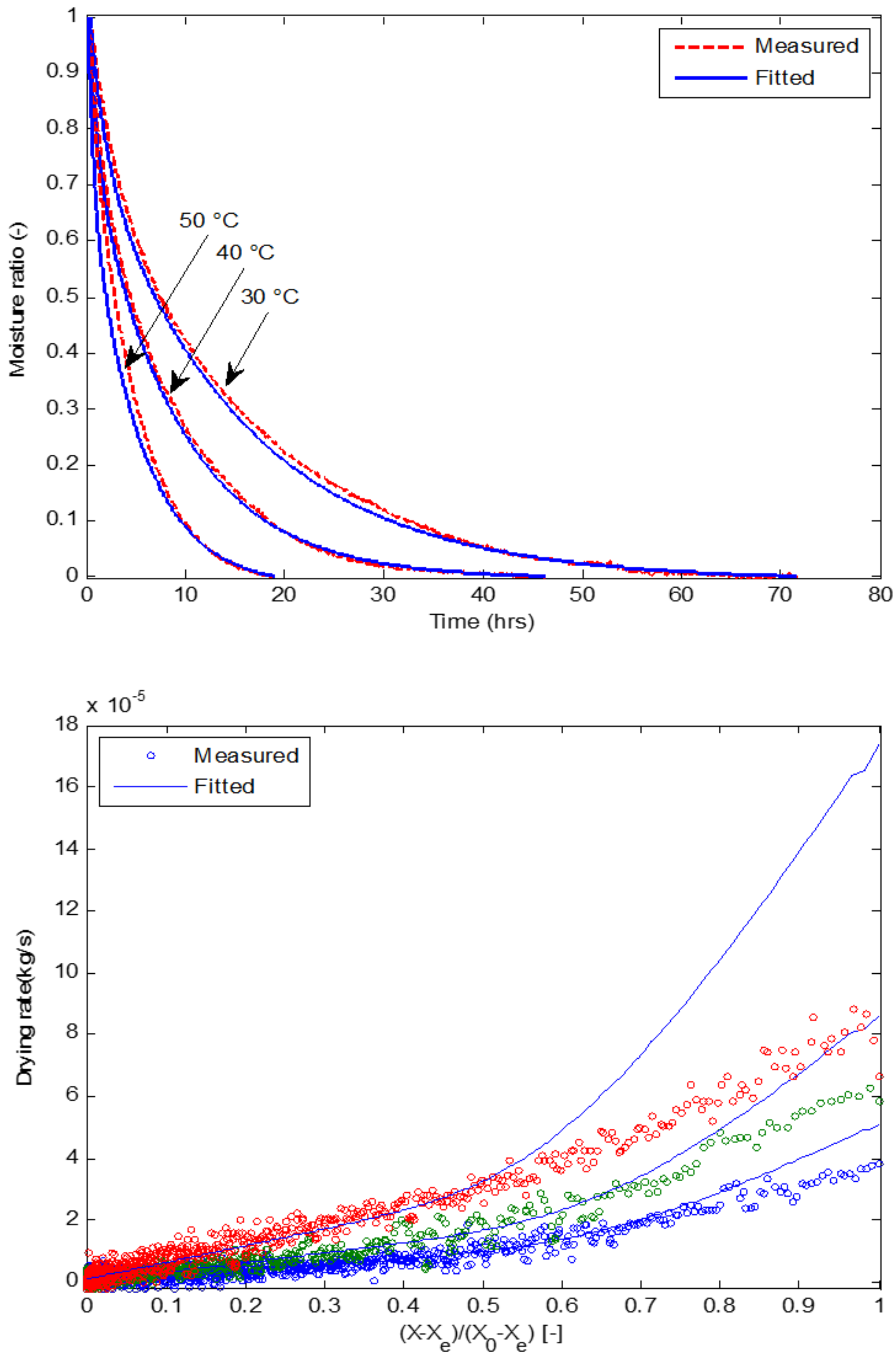

Fig 6. Results for the two term diffusion equation approximation. Moisture ratio as a function of time (top), drying rate as a function of moisture ratio (bottom) at constant slab thickness and diffusion coefficient.

Table 2 Estimated parameters with coefficient of variation in brackets (%) and statistical results for two-term at constant sample thickness and diffusion coefficient.

	Temperature °C	30	40	50
Two term equation at constant slab thickness and diffusion coefficient	$D \times 10^{-10}$ m^2/s	1.833 (0.22)	3.143 (0.28)	5.472 (0.93)
	p	0.301 (1.59)	0.300 (2.013)	0.434 (5.26)
	$MSe \times 10^{-4}$	0.577	0.553	0.694
	SE	0.007	0.007	0.0263
	PRD	2.987	3.306	15.707
	AIC	-3336.810	-2559.481	-508.501
	R^2	0.999	0.999	0.998

Because of the systematic deviations in both the drying curve and drying rate curve the effect of the dependency of L and D on X, is studied by considering four options. The results are given in Figure 7 and Table 3.

Option one: left graphs in Figure 7, concern a variable slab thickness, linearly related to the moisture content ($L(X) = c_1X(t) + c_2$, and based on Eq. (12), and a constant diffusion coefficient (D). The fits for the moisture ratio over time in Figure 7a and the drying rate in Figure 7b deviate significantly from the data, especially the drying curve.

Option two: Figure 7c,d, middle graphs, gives the results for an effective diffusion coefficient, linearly related to the moisture content according to $D(X) = D_0 + bX(t)$, in combination with a constant slab thickness. Compared to option 1, the drying curve with moisture ratio over time fits better to the data, which is also reflected by a lower mean squared error and standard error etc.

(see Table 3). Moreover, the drying rate model fits better to the data. However, the coefficient b in the expression $D(X) = D_0 + bX(t)$ is negative. This implies that the diffusion coefficient decreases with moisture content. In other words diffusive moisture transport becomes easier towards the end of drying, which is contradictory to the general experience from the literature [15].

Option three: Both sample thickness and diffusion coefficient are linearly related to the moisture content as presented in the previous options. The results are presented in Figure 7e,f (right graphs). In these graphs, the model results for the drying and drying rate curves are the closest to the data. The coefficient b in the expression $D(X) = D_0 + bX(t)$ is now positive which indicates a decreasing diffusion coefficient with decreasing moisture content. This result corresponds to a decline of water mobility during drying which corresponds to the general experience and which is amongst others explained by the free volume theory [16]. Compared with option 2, option 3 confirms the assertion by [17] that the diffusion coefficient varies during drying together with thickness. However, this option fails to predict well the observed data at high moisture content due to the accuracy level of the predictability of the initial relative length (Lc = 1.0).

Option four: Instead of Eq. 12, the fractal thickness of the sample as a function of moisture content from Eq. 15 is applied in combination of the effective diffusion coefficient, linearly related to the moisture content (see Figure 8). The parameters and fitting results are summarized in Table 3. The drying and the drying rate curves show similar fit with that of the third option but now with good prediction of the high initial moisture content.

Statistically, for the various temperatures, options 2, 3 and 4 are close and give the lowest MSe (10 fold or more lower), SE, PRD, AIC and higher R^2 compared to options 1. However option 2 is rejected for the fact that the coefficient of b is negative while option 4 is preferred over option 3 due to the good prediction of the high moisture region.

Actually, options three and four are very close and differ only in the way the thickness of the sample is related to the product moisture content. In option three, the relation was direct derived from the thickness data, while in option four the expression was based on the product volume. The last approach proved to be a more suitable method when dealing with non-infinite slabs and gives a better data smoothing result.

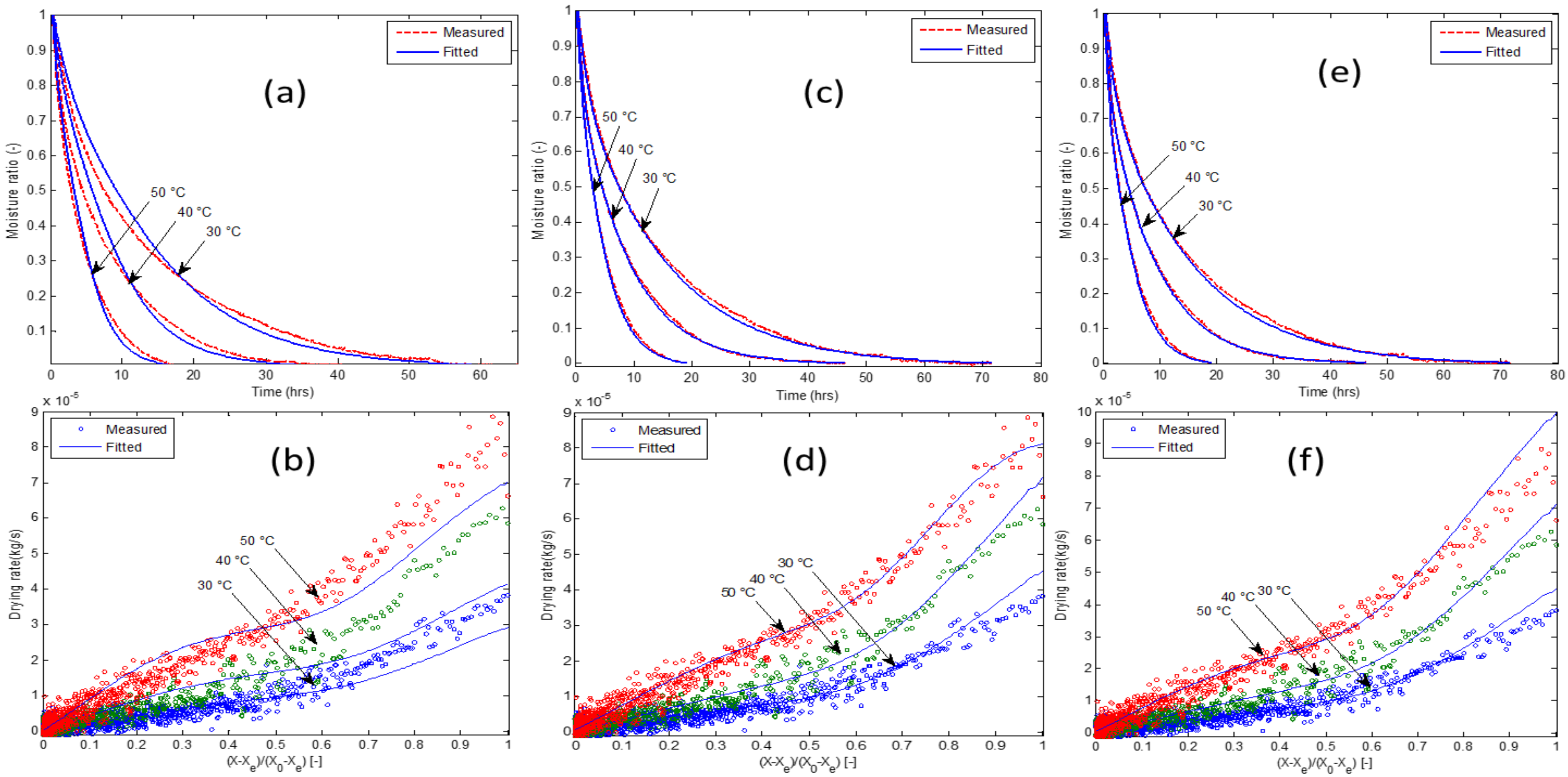

Figure 7 Results for the two term diffusion equation approximation (Eq. 16). Shrinkage as linear function of moisture content and constant diffusion coefficient (a,b). No shrinkage and diffusion coefficient as a linear function of moisture content (c,d). Combined effect of shrinkage and diffusion coefficient both linearly related with moisture content (e,f).

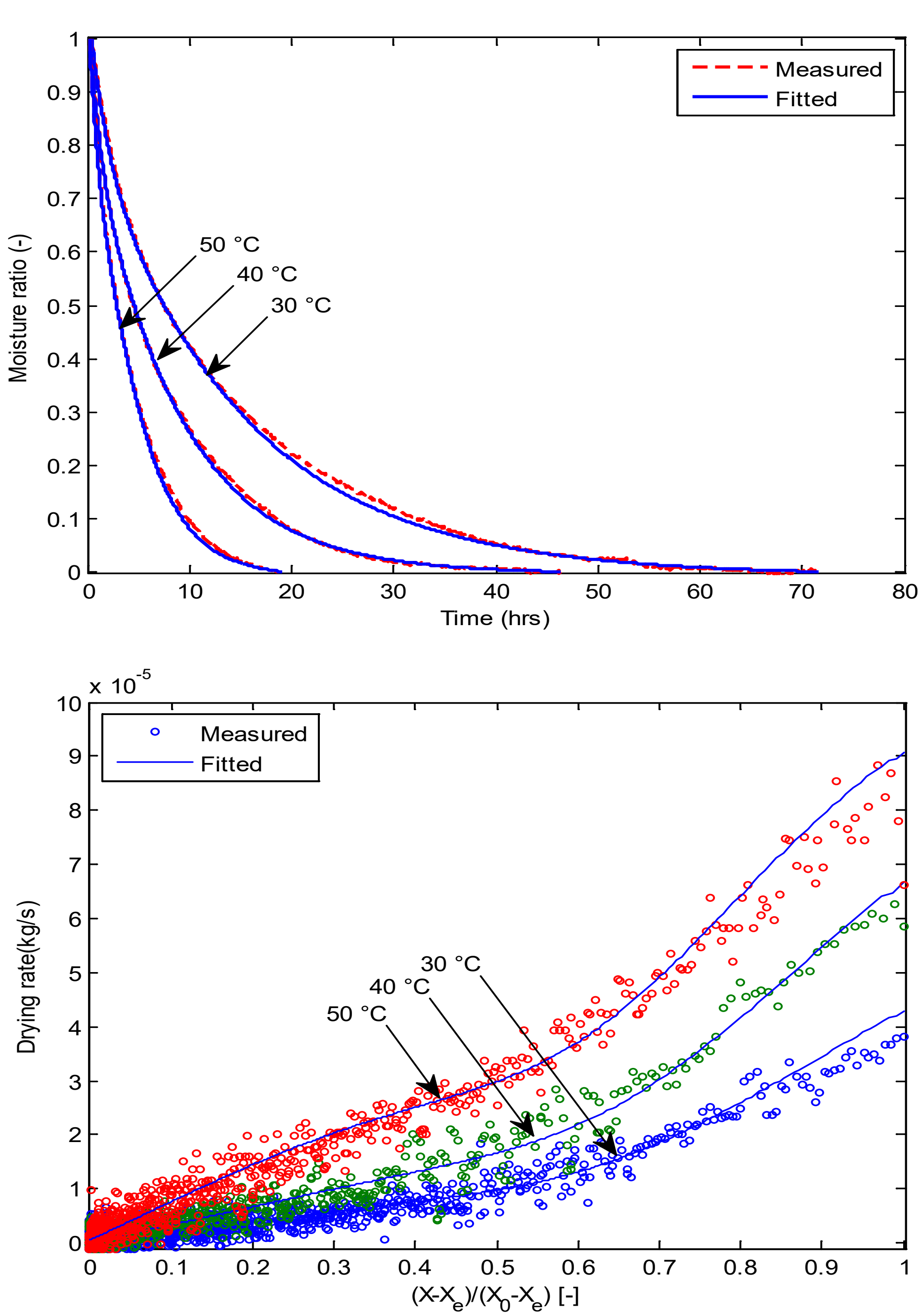

Figure 8 Results for the two term diffusion equation approximation (Eq. 16). Fractal thickness shrinkage (Eq.13) as a linear function of moisture content and diffusion coefficient linearly elated to moisture content. Top: Moisture as a function of time; Bottom: Drying rate as function of moisture content.

Table 2. Estimated parameters with coefficient of variation in brackets (%) and statistical results for the four model options.

	Temperature °C	30	40	50
Moisture content related slab thickness $L(X) = c_1X(t) + c_2$, Eq 12.	$D \times 10^{-10}$ m^2/s	1.117 (0.55)	1.850 (0.76)	2.914 (0.55)
	p	0.189 (4.30)	0.161 (6.87)	0.210 (3.72)
	$MSe \times 10^{-4}$	3.297	4.691	3.459
	SE	0.018	0.022	0.018
	PRD	3.224	4.186	5.326
	AIC	-1102.039	-780.727	-982.535
	R^2	0.999	0.998	0.999
Moisture content related diffusion coefficient $D(X) = D_0 + bX(t)$	$D_o \times 10^{-10}$ m^2/s	1.896 (0.40)	3.308 (0.36)	6.481 (0.38)
	$b \times 10^{-11}$	-0.899 (-9.72)	-2.461 (-5.86)	-15.069 (-1.87)
	p	0.276 (1.72)	0.261 (1.64)	0.245 (1.93)
	$MSe \times 10^{-4}$	0.447	0.224	0.404
	SE	0.007	0.005	0.006
	PRD	2.552	2.153	5.847
	AIC	-3669.424	-3251.979	-2443.452
	R^2	0.999	0.999	0.999
Combination of moisture related diffusion coefficient and slab thickness $L(X) = c_1X(t) + c_2$, Eq 12. $D(X) = D_0 + bX(t)$	$D_o \times 10^{-10}$ m^2/s	0.999 (0.47)	1.494 (0.45)	2.567 (0.45)
	$b \times 10^{-11}$	2.574 (2.48)	5.280 (1.81)	5.203 (3.04)
	p	0.272 (1.63)	0.257 (1.54)	0.279 (1.49)
	$MSe \times 10^{-4}$	0.436	0.231	0.2.97
	SE	0.007	0.005	0.005
	PRD	2.501	2.052	4.446
	AIC	-3693.266	-3283.395	-2652.928
	R^2	0.999	0.999	0.999
Combination of moisture related diffusion coefficient and fractal slab thickness $L(X)$: Eq 15. $D(X) = D_0 + bX(t)$	$D_o \times 10^{-10}$ m^2/s	1.008 (0.48)	1.506 (0.48)	2.607 (0.45)
	$b \times 10^{-11}$	2.490 (2.63)	4.953 (2.08)	4.250 (3.80)
	p	0.264 (1.69)	0.246 (1.71)	0.259 (1.57)
	$MSe \times 10^{-4}$	0.458	0.274	0.316
	SE	0.007	0.005	0.006
	PRD	2.593	2.271	5.044
	AIC	-3631.399	-3142.735	-2611.829
		0.999	0.999	0.999

3.5.Discussion

Mulet [12] emphasizes the role of shrinkage and varying diffusivity for the interpretation of drying curves. Ruiz-Lopez and Garcia-Alvarado[13] reported that a better estimation of effective diffusion coefficient can be achieved when both shrinkage and diffusivity as functions of moisture are factored in such models. In this work an additional analysis was made by examining curves of the drying rate as a function of moisture ratio. These curves show that the two-term approximation of the diffusion equation (equation 4) fit for the yam cubicles. The drying rate showed different stages during drying. Hassini et al. [5] modelled the stages by determining different values for the diffusion coefficient in each stage. In contrast to the work [5] in the current work the variation in diffusive transport is modelled by the two mechanisms: shrinkage and moisture dependent diffusion behavior. The moisture dependent diffusion behavior is attributed to the mobility of water in the product matrix, which is governed by the cell structure in yam and different water adsorption properties in mono and multilayers. Verma et al. [18] mentioned also starch gelatinization as possible reason for the variable diffusion behavior for product for temperatures beyond 65 ºC, but this level of temperature was not reached in this work.

The models with moisture dependent diffusion have one additional parameter (*b*). According to the lower AIC (Table 3) for those models, the addition of this extra parameter is justified. The two equations (12) and (15) do not differ much. However, in the interest of accurate prediction of the high moisture region preference is given to inclusion of the fractal shrinkage in the model.

The analytical expression for the diffusion in a slab as given by Crank explains the two apparent stages in the drying rate as a function of moisture ratio. These stages appear in a similar way for large infinite slabs as the smaller cubicles. The trend in these phases is strongly supported by the introduction of a sample moisture dependent thickness and diffusion coefficient in the model.

The mathematical form of the two-term approximation for Fick's diffusion equation as given in Eq. 16 corresponds to models used in semi-empirical expressions for the drying rate [18,19,20]. In those models the exponential terms are only estimated parameters. It is common practice to reject or to modify the mentioned models if the model does not adequately fit to the data. Examples of modifications are discussed in the review of [21]. Instead of modifying or seeking for another model, in this work the parameters were linked to moisture dependent diffusion behavior and shrinkage, which leads more to the fundamentals of moisture transport.

This work was focused on the mass transport by diffusion. From the dynamics for heat transfer a time constant around 30 seconds was derived. Therefore, the role of variations in temperature on the very slow mechanism of moisture transport can be neglected. The product samples remained close to the dryer inlet air temperature. Product quality degradation, like vitamin C and color were not the focus of this work. Vitamin C degradation which can already occur at the applied drying temperatures in the high moisture content region [22] needs attention in further investigation.

4. Conclusion

Crank's analytical solution of Fick's diffusion equation for slabs has been used to describe the drying behavior of yam (*Dioscoreaceae rotundata* cultivar *Dente*) in terms of moisture dependency of shrinkage and diffusivity. The analytical expression for the diffusion in a slab is also valid for the smaller cubicles, but results in a higher effective diffusion coefficient, and shows two stages in the drying rate as a function of moisture ratio.

The comparative study of moisture dependent shrinkage and moisture dependent diffusivity justifies the interdependence of diffusivity and shrinkage due to water loss during drying. This study shows that this behavior for yam is best explained by a combination of fractal moisture dependent shrinkage and moisture dependent diffusion. The moisture dependent diffusion behavior can be attributed to mobility of water from the food matrix due to different moisture content in the multilayer and monolayer regimes. The results from this study challenges to investigate the drying behavior of other food products.

Nomenclature

Symbols used for drying models

a, b, c_1, c_2, n	Constants
C_T, C_{T0}	Centre thickness of sample during drying and initial centre thickness (cm)
D	Effective diffusion coefficient (m^2/s)
D_0	Reference value for effective diffusion coefficient (m^2/s)
h	Height of parabolic inclination at top and bottom of sample (m)
$L, L(X)$	Thickness of yam samples and thickness as a function of moisture content (m)
L_i, L_0	Measured sample thickness during drying, and initial sample thickness (m)
L_c	Relative thickness (-)
$MR(t)$	Moisture ratio (-)
p	Second term pre-exponential coefficient of the two term diffusion equation

r	Radius of parabolic inclination at top and bottom of sample (m)
S_T, S_{T0}	Side thickness of sample and initial side thickness (cm)
S_L, S_{L0}	Side length of a sample and initial side length (cm)
t	Time (s)
V_i, V_0	Measured sample volume during drying, and initial sample volume (m^3)
V_c	Relative volume (-)
V_{sqr}, V_{par}	Volume of rectangular part of sample, volume of parabolic inclination at top and bottom of sample (m)
x	Position in the product compared to the center (m)
$X(t)$	Moisture content during drying (kg water/kg dry matter)
X_0, Xe	Initial and equilibrium moisture content (kg water/kg dry matter)
z	Fractal coefficient (-)

Symbols used for statistics

AIC	Aikaike information criterion
MSe	Mean squared error
N_e	Number of data points
N_p	Number of parameters
PRD	Percentage relative deviation
$Residuals$	Not yet given
SE	Standard error
$V(\hat{p})$	Sum of squared errors
$\bar{X}$	Mean value

Acknowledgement

This project was funded by the Wageningen University and Research Centre (WUR), The Netherlands and Kwame Nkrumah University of Science and Technology (KNUST), Kumasi, Ghana. The authors are grateful for this financial and consumables contribution.

References

[1] Fioreze, R., Morini, B. Yam (Discorea sp) Drying with different cuts and temperatures: experimental and simulated results. Ciencia Technology, Alimentos. 2000, 20, 262–266.

[2] Torres, R., Montes, E.J., Andrade, R.D., Perez, O.A., Toscano, H. Drying kinetics of two yam (*Dioscoreaceae alata*) varieties. Dyna. 2011, 79(171), 175-182.

[3] Yadollahinia, A. Jahangiri, M. (2009) Shrinkage of potato slice during drying, Journal of Food Engineering 94, 52–58.

[4] Al-Muhtaseb, A.H., McMinn, W.A.M., Magee, T.R.A., 2004. Shrinkage, density and porosity variations during the convective drying of potato starch gel. In: 14th International Drying Symposium (IDS), São Paulo, Brazil, vol. C, pp. 1604–1611. Eds. M.A. Silva, Campinas State University, Brazil.

[5] Hassini, L., Azzouz, S. Peczalski, R. Belghith, A. Estimation of potato moisture diffusivity from convective drying kinetics with correction for shrinkage, Journal of Food Engineering 2007, 79, 47–56

[6] Sjöholm, I. and Gekas, V. Apple Shrinkage upon Drying, Journal of Food Engineering. 1995, 25, 123-130.

[7] Crank, J. The Mathematics of Diffusion. 1975. Oxford University Press. Oxford.

[8] Ah-Hen, K.,Zambra, C.E.,Aguëro, J.E.,Vega-Gálvez, A.,Lemus-Mondaca,R., Moisture diffusivity coefficient and convective drying modelling of murta (Ugni molinae Turcz): Influence of temperature and vacuum on drying kinetics. Food and Bioprocess Technology (2013) 6(4) 919-930.

[9] Ben Haj Said, L., Najjaa, H., Farhat, A., Neffati, M., & Bellagha, S. (2015). Thin layer convective air drying of wild edible plant (Allium roseum) leaves: experimental kinetics, modeling and quality. Journal of Food Science and Technology, 52(6), 3739–3749.

[10] *Chayjan,* R.A., Salari K, Barikloo H. Modeling moisture diffusivity, activation energy and specific energy consumption of squash seeds in a semi fluidized and fluidized bed drying Acta Sci Pol Technol Aliment. 2012, 11(2):131-48.

[11] Asiah, N., Djaeni, M., Hii, C.L. Moisture transport mechanism and drying kinetic of fresh harvested red onions bulbs under dehumidified air. International Journal of Food Engineering, 2017. DOI:10.1515/ijfe-2016-0401

[12] Mulet, A. Drying modelling and water diffusivity in carrots and potatoes. Journal of Food Engineering, 1994, 22, 329–348.

[13] Ruiz-Lopez. I.I., Garcia-Alvarado M.A. Analytical solution for food-drying kinetics considering shrinkage and variable diffusivity. Journal of Food Engineering. 2007,79: 208-216.

[14] Gekas, V.; Lamberg, I. Determination of Diffusion Coefficients in Volume-Changing Systems - Application in the Case of Potato Drying Journal of Food Engineering. 1991, 14, 317-326.

[15] Jannot, Y., Talla, A., Nganhou, J., Puiggali, J.R. Modeling of banana convective drying characteristic curve (DCC) method. Drying Technology. 2004, 22, 1949-1968.

[16] Jin X., Sman, R.G.M.van der, Boxtel A.J.B. van. Evaluation of the Free Volume Theory to predict moisture transport and quality changes during broccoli drying. Drying Technology. 2011, 29(16),1963-1971.

[17] Tütüncü, M.A., Labuza, T. P. Effect of Geometry on the Effective Moisture Transfer Diffusion Coefficient, Journal of Food Engineering. 1996, 30, 433-447.

[18] Verma L.R., Bucklin R.A., Endan J.B., Wratten F.T. Effect of drying air parameters on rice drying models. Transaction of the ASAE, 1985, 28(1), 296-301.

[19] Henderson, S.M. Progress in developing the thin layer drying equation. Transactions of the ASAE 1974,17,1167-1172.

[20] Sharaf-Eldeen, Y.I., Blaisdell, P.N., Hamdy , M.Y. A model for corn drying. Transactions of the ASAE 1980,23,1261-1271.

[21] Erbay, Z., Icier, F. A review of thin layer drying of foods: Theory, modelling, and experimental results. Critical Reviews in Food Science and Nutrition. 2010, 50:5,441-464.